Scanning Plasmon Near-Field Microscope

M. Specht, J. D. Pedarnig, W. M. Heckl, and T. W. Hänsch
Sektion Physik der Universität München, Schellingstrasse 4/III, D-8000 München 40, Germany
(Received 28 October 1991)

A new optical near-field microscope with a lateral resolution of 3 nm ($\lambda/200$) is presented. Resonantly excited extended surface plasmons generate an optical near field which is locally probed by a sharp tip. The interaction of the surface plasmons with the tip can be understood in terms of elastic plasmon scattering and radiationless energy transfer from the tip to the sample. The new technique may permit the detection and spectroscopic identification of single adsorbed molecules.

PACS numbers: 42.30.Hn, 07.60.Pb, 73.20.Mf

The resolving power of classical optical microscopes is restricted by Abbe's diffraction limit to about one-half of the optical wavelength. However, it is possible to overcome this limit. If a subwavelength hole in a metal sheet is scanned close to an object, a super-resolved image can be built up from the detected light that passes through the hole. Scanning optical near-field microscopy based on this principle was first proposed by Synge [1] and demonstrated at microwave frequencies ($\lambda = 3$ cm) by Ash and Nicholls with a resolution of $\sim\lambda/60$ [2]. At visible wavelengths several different probes have been developed over the last decade that yield super-resolution capabilities [3–6].

Here we report on a new type of near-field microscope where we have demonstrated an order-of-magnitude increase in lateral resolution to 3 nm ($\lambda/200$) at optical wavelengths. The scanning plasmon near-field microscope (SPNM) (Fig. 1) is based on the interaction of extended surface plasmons (SP), as introduced by Ritchie [7], with a sharp metal tip which is placed close to the surface of the object. Theoretical considerations indicate that this interaction can be understood mainly in terms of elastic plasmon scattering as well as radiationless energy transfer from the tip to the sample. These processes depend very strongly on the distance between tip and sample and are the key for a high lateral resolution capability. By raster scanning the tip over the sample surface, nanometer-scale maps of interaction strength (related to the topography of the sample) can be recorded.

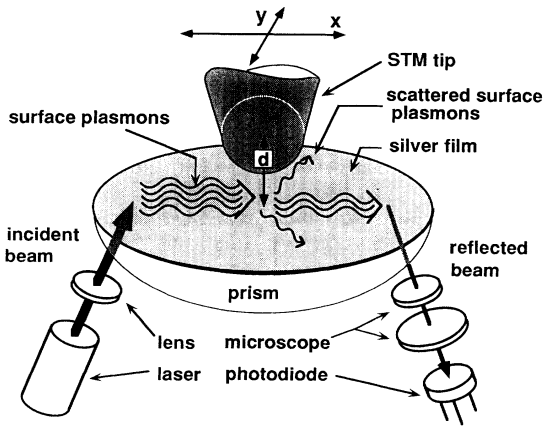

FIG. 1. Scheme of the experiment: Surface plasmons, excited by an incident laser beam, interact with a thin tungsten tip positioned very close to a silver surface.

In the SPNM the tip is scanned a few nm above the sample, where the mechanical forces are small. SPNM may therefore permit an essentially nonperturbative method of microscopy in contrast to scanning tunneling microscopy (STM) and atomic force microscopy [8], where large forces (see Ref. [9]) can lead to significant perturbation and sample damage. In addition to the topography the electromagnetic nature of the interaction should permit spectroscopic information to be obtained. Thus the SPNM may give a powerful tool for chemical identification on a molecular scale due to its high resolution, low probing forces, and spectroscopic capability.

The experimental setup contains three microscopes on different scales: an STM using the stylus as a tunneling tip, the SPNM using the stylus as an optical near-field sensor, and an optical microscope [10]. Consequently the setup allows for overlapping and complementary *in situ* characterization of the sample over many orders of magnitude (0.1 nm to 1 mm).

In the exploratory experiments reported here, a silver film evaporated onto a glass prism serves as the sample. The preparation follows a standard technique (high vacuum, $p < 10^{-5}$ mbar, room temperature, evaporation rate of 0.5 nm/sec, and final mass thickness 50 nm). All measurements have been made under ambient conditions immediately after preparing the film in order to avoid possible aging effects. The tungsten stylus has been prepared by electrochemical dc etching yielding tips with radii of curvature of about 10 nm. The incident laser light is coupled to the SP mode at the silver-air interface via a prism in the usual Kretschmann configuration [11–13]. The excitation of SP is recognized as a minimum in the reflected light intensity [attenuated total reflection (ATR) minimum] [13] and can be understood as destructive interference between the light reflected from the silver-air and the glass-silver boundaries.

The laser beam is polarized parallel to the plane of in-

cidence and is focused onto the base of the prism (focal length, 150 mm; spot size, $\sim 200\ \mu m$). For efficient coupling the beam divergence has to remain below the SP excitation half-width. The reflected light is directed into an optical microscope (magnification 25×, numerical aperture 0.07), imaging the area where the tip touches the surface. An aperture preselects the reflected light from the relevant area on the surface. Moving the tungsten tip nearer to the silver surface slightly enlarges the reflected light intensity, because the destructive interference is reduced, thus yielding a distance-dependent signal. The intensity changes are measured with a photodiode. The experiments have been carried out with a He-Ne laser ($\lambda = 632.8$ nm, $I = 1$ mW) and a He-Cd laser ($\lambda = 441.7$ nm, $I = 10$ mW). The signal-to-noise ratio could be improved by using some polarization optics similar to a scheme used in polarization spectroscopy [14].

The super-resolution capability of the near-field microscope is very well demonstrated in a series of four images (Fig. 2). These pictures are all taken at the same place and show the topography of a silver surface on a scale of 600 nm×600 nm. Figure 2(a) shows an STM image of this area recorded in the constant-current mode. The most significant feature is a small hole produced by pressing the tip slightly into the silver surface. The intrinsic surface corrugation exhibits an "island structure" with a mean diameter of about 20 nm.

An optical near-field image with an average tip-to-sample spacing of 3 nm is shown in image 2(b). The hole can be imaged with a resolution comparable to the STM image, 2(a). Moreover, there are two additional features: a wavy structure that has a periodicity comparable to the size of the granular silver surface and some larger "blobs" that might be caused by either standing plasmon waves or long-range surface inhomogeneities. This image has been recorded in a controlled constant-height mode that compensates for piezo and thermal drifts. After each line scan the tip approaches the surface using the tunneling point as zero reference. Image 2(c) has been recorded at a distance of 10 nm with the same imaging mode. The hole appears smeared out, the wavy structure has disappeared, and only the larger blobs remain detectable. As one expects, an increase in tip-to-sample spacing reduces the resolution. Image 2(d) is recorded from the optical signal while a tunneling current between tip and sample is held at a constant value. The lateral resolution in this "STM-SPNM hybrid mode" is not purely optical in origin. However, one can observe enhanced contrast along the island boundaries compared with the pure STM picture.

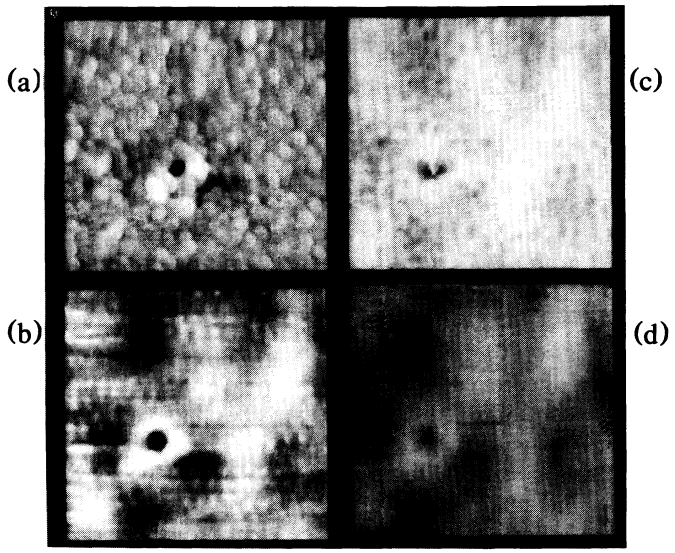

FIG. 2. (a) STM image taken at a 600 nm×600 nm area on a silver surface (tip-sample spacing below 1 nm); (b),(c) SPNM images taken at the same area (tip-sample spacing 3 and 10 nm, respectively; wavelength 632.8 nm); (d) image recorded in the "STM-SPNM hybrid mode" (tip-sample spacing below 1 nm).

A quantitative comparison of the STM and the SPNM images of the hole permits an estimation of the lateral resolution of the SPNM. Using the STM image as a reference, the mean deviation of the SPNM trace at the edges of the hole yields a value $\langle \delta x \rangle \approx 3$ nm (Fig. 3). Imaging appears to work better after slightly touching the sample with the tip, possibly depositing silver on it. One can envision engineered compound tips with optimized imaging characteristics. An interesting probe may be an insulating needle with a single resonant molecule at the tip.

To get an understanding of the imaging mechanism we concentrate on what happens if the distance d between tip and sample is varied. The explanation of the detailed form of the distance-dependent reflection curve (Fig. 4) is a good starting point for theoretical considerations. To first order one expects that the tip acts as a scattering center for the incoming surface plasmons. The nonspecular scattered intensity should be proportional to the square of the unperturbed SP field at the tip. This would

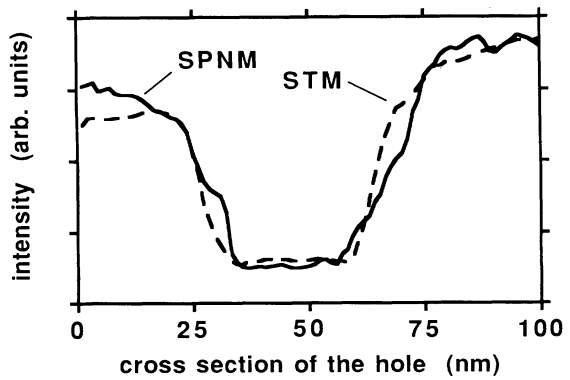

FIG. 3. Cross section through the hole of Figs. 2(a) and 2(b).

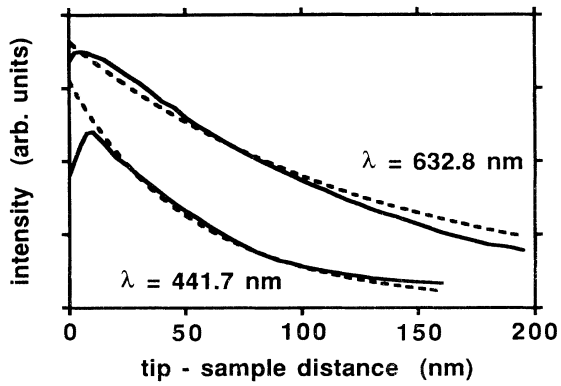

FIG. 4. Reflected intensity vs tip-to-sample distance. Zero distance is defined by tunneling contact of the tip. The experimental curves (solid lines) are compared with $P(\gamma)$ (dashed lines) for two different wavelengths in the low damping limit.

give an exponential decay law proportional to $E_0^2 T \times \exp(-2k_z d)$, where $k_z = (2\pi/\lambda)(\varepsilon'_{Ag}+1)$ is the inverse decay length of the evanescent SP field in the air, T is the SP enhancement factor [13], and E_0^2 is the incident laser intensity.

However, the experimental distance curves (Fig. 4) show a much shorter decay length and a strong decrease in the reflected intensity when the tip comes very close to the surface. A better theoretical description therefore has to take into account that the field at the tip is a superposition of the unperturbed SP field E and the scattered field E_r reflected from the silver surface. We can visualize the back reaction of the reflected field as an example of the radiation-reaction damping of classical electrodynamics. Following Sommerfeld [15] and Chance, Prock, and Silbey [16] we simulate the tip in a simple model by an oscillating dipole p with charge e and effective mass m, where the fields E and E_r act as the driving forces:

$$\ddot{p} + \gamma_0 \dot{p} + \omega_0^2 p = (e^2/m)(E + E_r) . \quad (1)$$

In the absence of any external force, γ_0 is the damping constant and ω_0 is the resonance frequency of the free oscillator. The real part of the reflected field E_r (in phase with the dipole) and the imaginary part of E_r (out of phase with the dipole) cause a shift in resonance frequency and additional damping, respectively. The shift in resonance frequency turns out to be almost negligible [16], whereas the total normalized damping becomes

$$\frac{\gamma}{\gamma_0} = 1 + \frac{3}{2} q \, \mathrm{Im}\left[\int_0^\infty r_p \exp(-2\kappa l d) \frac{u^3}{v} du\right] . \quad (2)$$

The integral is valid for a dipole oriented perpendicular to the surface and represents the Fourier sum of radial waves in cylindrical coordinates, with the variable u being the k vector normalized with respect to the free photon k vector κ in air; r_p is the amplitude reflection coefficient for p-polarized light, $v = (u^2 - 1)^{1/2}$, and $q = \gamma_r/\gamma_0$, where γ_r is the radiation damping of the free oscillator.

As shown in Ref. [17], for perfectly flat surfaces the effect of the metal on the damping can be split into four terms representing different physical mechanisms:

$$\gamma/\gamma_0 = 1 + q(D_{\mathrm{intf}} + D_{\mathrm{abs}} + D_{\mathrm{SP}} + D_{\mathrm{LSW}}) . \quad (3)$$

Here D_{intf} and D_{abs} come from the region $0 < u < 1$ and represent the interference between direct and reflected fields and the absorption of photons in the metal. These terms have only a slight distance dependence. The reflection coefficient r_p has a pole which represents the excitation of SP [13] and D_{SP} depends on the distance as $D_{\mathrm{SP}} \sim \exp(-2k_z d)$. At distances from 10 to 200 nm, energy transfer through SP excitation is a very important mode of decay. The contribution D_{LSW} comes from the continuum of high momentum lossy surface waves which are predominantly excited when the dipole is very close to the metal (< 10 nm) and exhibits an inverse cubic distance dependence [16].

In our experiment we measure the dissipated energy of the oscillator $P(\gamma)$ corresponding to a change in the reflected light intensity,

$$\frac{P(\gamma)}{P(\gamma_0)} = T \exp(-2k_z d) \frac{\gamma}{\gamma_0} \frac{(\omega_0^2 - \omega^2)^2 + \omega^2 \gamma_0^2}{(\omega_0^2 - \omega^2)^2 + \omega^2 \gamma^2} . \quad (4)$$

In the case of low damping $\gamma \sim \gamma_0$ and the frequency ω being far off the resonance frequency ω_0, the absorbed power $P(\gamma)$ increases proportionally to γ/γ_0. In this range the scattering into SP and the sum of radiation damping and photon absorption are about equally important and contribute to the exponential distance dependence of $P(\gamma)$ with a decay length of $(4k_z)^{-1}$ and $(2k_z)^{-1}$, respectively. For very small separations ($d < 10$ nm) the nonradiative energy transfer dramatically increases the damping ($\gamma \gg \gamma_0$, due to D_{LSW}) and $P(\gamma)$ decreases proportionally to $1/\gamma$. The transition between these two regions causes a maximum in the distance dependence of $P(\gamma)$ that depends on ω, ω_0, and γ_0. The signal scales with the SP enhancement factor T which depends on the dielectric constant of the substrate material. It is largest for silver (at $\lambda = 600$ nm, $T \sim 200$) but still reasonably high for other metals like, e.g., aluminum (at $\lambda = 600$ nm, $T \sim 40$) [13].

Equation (4) allows the comparison of the experimental and theoretical results (Fig. 4 shows theoretical curves in the case of low damping). For tip-sample spacings between 20 and 200 nm the normalized calculated power absorption agrees to within 15% with the measured reflection curve. For shorter spacings the strong decrease in the reflected intensity can be qualitatively understood because of radiationless energy transfer from the tip to the film. This process has an even stronger distance dependence ($\sim d^3$) than the pure exponential behavior and may be the main reason for the high lateral resolution capability of the SPNM.

We now would like to suggest how radiationless energy

transfer can be used to observe locally single-molecule resonances. In order to avoid strong damping from the metal surface the molecule should be positioned at least several nanometers away from the surface. In resonance the power absorption from the incoming SP [Eq. (4) is also valid for a molecule] is proportional to $1/\gamma$. If a tip scans over the molecule its oscillation is strongly damped due to radiationless energy transfer to the tip. The strongly enhanced damping changes the reflectivity for the incident light. Assuming that the scattering cross section of the molecule $\sigma(\omega_0) \approx 0.01\ \mathrm{nm}^2$ is then reduced to zero causes a change in the reflected light intensity by about $\Delta I = [(0.01\ \mathrm{nm}^2)/A] T I_0$, where A is the area of the laser spot on the sample. With our experimental parameters this value is 0.2 pW, which corresponds to about 1% of the influence of the tip itself. Therefore the local detection of single-molecule resonances should become achieveable.

In summary, the studies reported here demonstrate that the interaction of SP with a sharp tip, positioned in their evanescent field, provides a method to investigate sample surfaces with subwavelength super-resolution. Images of silver surfaces with a lateral resolution of 3 nm demonstrate the potential of this method. In addition there is evidence that elastic plasmon scattering and radiationless energy transfer from the tip to the sample are the main physical processes responsible for the high resolution. Finally our detection technique is a promising method for local spectroscopy of single adsorbed molecules.

We would like to thank very much J. Holzrichter for stimulating discussions and the Deutsche Forschungsgemeinschaft (Ha 1457/1-2) for partly supporting this work.

[1] E. H. Synge, Philos. Mag. **6**, 356 (1928).
[2] E. A. Ash ad G. Nicholls, Nature (London) **237**, 510 (1972).
[3] A. Lewis *et al.*, Ultramicroscopy **13**, 227 (1984).
[4] D. W. Pohl, W. Denk, and M. Lanz, Appl. Phys. Lett. **44**, 651 (1984).
[5] R. C. Reddick, R. J. Warmack, and T. L. Ferrell, Phys. Rev. B **39**, 767 (1989).
[6] E. Betzig *et al.*, Science **251**, 1468 (1991), and references quoted therein.
[7] R. H. Ritchie, Phys. Rev. **106**, 874 (1957).
[8] G. Binnig and H. Rohrer, IBM J. Res. Dev. **30**, 355 (1986).
[9] U. Dürig, J. K. Gimzewski, and D. W. Pohl, Phys. Rev. Lett. **57**, 2403 (1986).
[10] B. Rothenhäusler and W. Knoll, Nature (London) **332**, 615 (1988).
[11] A. Otto, Z. Phys. **216**, 398 (1968).
[12] E. Kretschmann, Z. Phys. **241**, 313 (1971).
[13] H. Raether, *Surface Plasmons*, Springer Tracts in Modern Physics Vol. 111 (Springer, Berlin, 1988).
[14] C. Wieman and T. W. Hänsch, Phys. Rev. Lett. **36**, 1170 (1976).
[15] A. Sommerfeld, *Partial Differential Equations in Physics* (Academic, New York, 1949), Chap. 4.
[16] R. R. Chance, A. Prock, and R. Silbey, in *Advances in Chemical Physics*, edited by I. Prigogine and S. A. Rice (Wiley, New York, 1978), Vol. 37, p. 1.
[17] W. H. Weber and C. F. Eagen, Opt. Lett. **4**, 236 (1979).

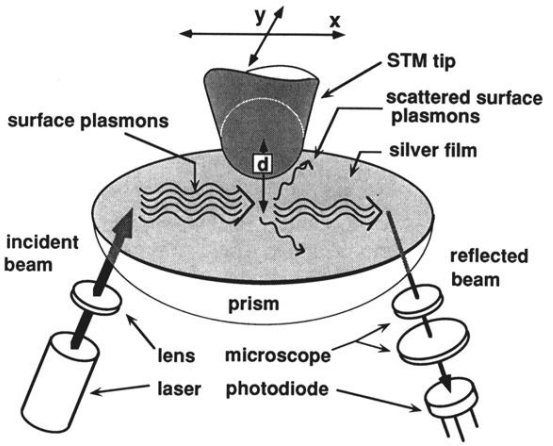

FIG. 1. Scheme of the experiment: Surface plasmons, excited by an incident laser beam, interact with a thin tungsten tip positioned very close to a silver surface.

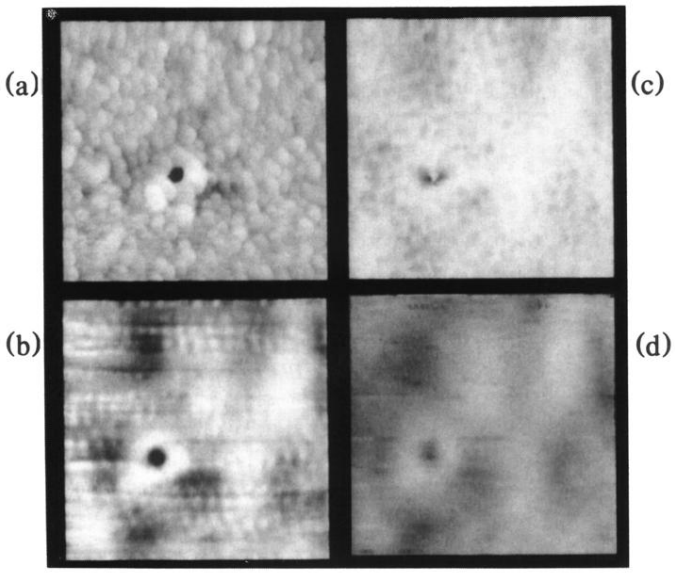

FIG. 2. (a) STM image taken at a 600 nm×600 nm area on a silver surface (tip-sample spacing below 1 nm); (b),(c) SPNM images taken at the same area (tip-sample spacing 3 and 10 nm, respectively; wavelength 632.8 nm); (d) image recorded in the "STM-SPNM hybrid mode" (tip-sample spacing below 1 nm).